

High Performance and Cycling Stability Supercapacitors Employing MnS@Polypyrrole Nanocomposites as Cathode Material

Mahir GÜLEN^{1*} 

¹Bartın University, Faculty of Engineering, Architecture and Design, Department of Mechanical Engineering, 74100, Bartın, Turkey

Article Info:

Research article
Received: 07/01/2023
Revision: 22/02/2023
Accepted: 23/03/2023

Keywords

Energy storage
Supercapacitor
Nanocomposites
Renewable energy

Makale Bilgisi

Araştırma makalesi
Başvuru: 07/01/2023
Düzeltilme: 22/02/2023
Kabul: 23/03/2023

Anahtar Kelimeler

Enerji depolama
Süperkapasitör
Nanokompozitler
Yenilenebilir enerji

Graphical/Tabular Abstract (Grafik Özet)

In this study, a nanocomposite is prepared to obtain supercapacitor with high specific capacitance and cycling stability. The nanocomposite is fabricated by the electropolymerization of PPy on MnS, following synthesis of MnS via rapid and simple microwave-assisted method / Bu çalışmada, yüksek özgül kapasitans ve çevrim kararlılığına sahip süperkapasitör elde etmek için bir nanokompozit hazırlanmıştır. Nanokompozit, MnS'nin hızlı ve basit mikrodalga destekli yöntemle sentezinin ardından PPy'nin MnS üzerine elektropolimerizasyonu ile üretilmiştir.

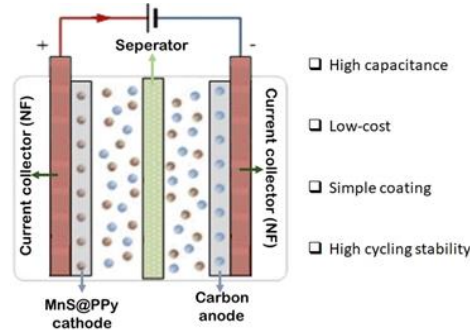


Figure A: Schematic diagram of prepared supercapacitor / Şekil A: Hazırlanan süperkapasitörün şematik diyagramı

Highlights (Önemli noktalar)

- MnS@PPy nanocomposite/MnS@PPy nanokompozit
- High capacitance/Yüksek kapasitans
- High stability/Yüksek kararlılık

Aim (Amaç): In this research, to increase the electric conductivity, cycle life stability, electro-activity and capacitance of PPy, MnS have been incorporated into PPy matrix and resulting nanocomposite employed as cathode material in supercapacitors / Bu çalışmada, PPy'nin elektrik iletkenliğini, çevrim ömrü kararlılığını, elektro-aktivitesini ve kapasitansını artırmak için MnS, PPy matrisine dahil edilmiş ve elde edilen nanokompozit, süperkapasitörlerde katot malzemesi olarak kullanılmıştır.

Originality (Özgünlük): MnS was synthesized using microwave assisted method and incorporated into PPy matrix for the first time to prepare MnS@PPy nanocomposite with high cycling stability and electrocatalytic activity / MnS, mikrodalga destekli yöntem kullanılarak sentezlenmiş ve ilk kez yüksek çevrim kararlılığı ve elektrokatalitik aktiviteye sahip MnS@PPy nanokompozit hazırlamak için PPy matrisine dahil edilmiştir.

Results (Bulgular): By incorporation of MnS into PPy matrix, the electrochemical and stability of PPy are improved. These improvements can be attributed to i) the increase in conductivity of nanocomposite stem from the synergistic effect between MnS and PPy, ii) the enlargement of the active surface area, iii) the increase in the ion diffusion rate, iv) the improvement of charge transfer kinetics and v) the increase in stability against volume change / MnS'nin PPy matrisine dahil edilmesiyle PPy'nin elektrokimyasal ve kararlılığı iyileştirilir. Bu iyileştirmeler; i) MnS ve PPy arasındaki sinerjistik etkiden nanokompozit gövdenin iletkenliğindeki artışa, ii) aktif yüzey alanının genişlemesine, iii) iyon difüzyon hızındaki artışa, iv) yük transfer kinetiğinin iyileştirilmesine ve v) hacim değişikliğine karşı stabilitenin artışına atfedilebilir.

Conclusion (Sonuç): The MnS@PPy electrode exhibited a capacitance about 5.6 times higher than bare PPy as well as a higher cycling stability. In the light of the obtained results, it can be said that the MnS@PPy structured nanocomposite is a promising candidate for commercialization of SC applications / MnS@PPy elektrodu, saf PPy'den yaklaşık 5,6 kat daha yüksek bir kapasitans ve ayrıca daha yüksek bir çevrim kararlılığı sergilemiştir. Elde edilen sonuçlar ışığında, MnS@PPy yapılı nanokompozitin SC uygulamalarının ticarileştirilmesi için umut vadeden bir aday olduğu söylenebilir.



High Performance and Cycling Stability Supercapacitors Employing MnS@Polypyrrole Nanocomposites as Cathode Material

Mahir GÜLEN^{1*}

¹Bartın University, Faculty of Engineering, Architecture and Design, Department of Mechanical Engineering, 74100, Bartın, Turkey

Article Info

Research article
Received: 07/01/2023
Revision: 22/02/2023
Accepted: 23/03/2023

Keywords

Energy storage
Supercapacitor
Nanocomposites
Renewable energy

Abstract

In this study, MnS metal sulphide was incorporated into polypyrrole (PPy) matrix, and the fabricated nanocomposites were used for the first time as active electrode in supercapacitor (SC) architecture. MnS was obtained in a short time (15 min) via simple microwave technique, and the nanocomposite was synthesised successfully with electropolymerization of PPy in presence of MnS on nickel foam. Incorporation of MnS changed the growth mechanism of PPy, leading to increase in surface area, electrocatalytic activity and conductivity of the resulted nanocomposites. More importantly, MnS@PPy electrode exhibited a specific capacitance (C_s) of 1102 F/g which is approximately 5.6 times higher than that of the bare PPy (197 F/g). Furthermore, energy density (E_d) of the bare PPy was determined as 4.37 W/kg, by incorporation of MnS into PPy matrix the E_d value increased to 24.5 W/kg. On the other hand, after 1000 charge/discharge cycles, the cycle stability of the bare PPy remained at 72%, while MnS@PPy nanocomposite electrode is 95 %. The reasons for these improvements can be listed as; i) the increase in conductivity of nanocomposite stem from the synergistic effect between MnS and PPy, ii) the enlargement of the active surface area, iii) the increase in the ion diffusion rate, iv) the improvement of charge transfer kinetics and v) the increase in stability against volume change. In the light of the results obtained from this study, it can be said that the MnS@PPy structured nanocomposite is a promising candidate for commercialization of SC applications.

Katot Malzemesi olarak MnS@Polipirol Nanokompozitleri İçeren Yüksek Performans ve Döngü Kararlılığına Sahip Süper Kapasitörler

Makale Bilgisi

Araştırma makalesi
Başvuru: 07/01/2023
Düzeltilme: 22/02/2023
Kabul: 23/03/2023

Anahtar Kelimeler

Enerji depolama
Süperkapasitör
Nanokompozitler
Yenilenebilir enerji

Öz

Bu çalışmada MnS metal sülfür, polipirol (PPy) matrisine eklenmiş ve elde edilen nanokompozitler ilk kez süper kapasitör (SC) mimarisinde aktif katot olarak kullanılmıştır. MnS, basit mikrodalga tekniği ile kısa sürede (15 dakika) sentezlenmiş ve polipirol (PPy) de elektropolimerizasyon yöntemi ile MnS varlığında nikel köpük üzerine kaplanarak nanokompozitler başarıyla hazırlanmıştır. MnS'nin yapıya dahil edilmesi, PPy'nin büyüme mekanizmasını değiştirerek, elde edilen nanokompozitlerin yüzey alanında, elektrokatalitik aktivitesinde ve iletkenliğinde artışa yol açmıştır. Daha da önemlisi, MnS@PPy elektrodu, saf PPy'den (197 F/g) yaklaşık 5,6 kat daha yüksek olan 1102 F/g'lik bir spesifik kapasitans (C_s) sergilemiştir. Ayrıca saf PPy'nin enerji yoğunluğu (E_d) 4,37 W/kg olarak belirlenmiş, MnS'nin PPy matrisine katılmasıyla E_d değeri 24,5 W/kg'a yükselmiştir. Öte yandan, 1000 şarj/deşarj döngüsünden sonra saf PPy'nin döngü kararlılığı %72'de kalırken, MnS@PPy nanokompozit elektrot için %95'tir. Bu iyileştirmelerin nedenleri; i) MnS ve PPy arasındaki sinerjistik etkiden nanokompozit gövdenin iletkenliğindeki artış, ii) aktif yüzey alanının genişlemesi, iii) iyon difüzyon hızındaki artış, iv) yük transfer kinetiğinin iyileştirilmesi ve v) hacim değişikliğine karşı kararlılık sergilenmesi olarak sıralanabilir. Bu çalışmadan elde edilen sonuçlar ışığında, MnS@PPy yapıları nanokompozitin SC uygulamalarının ticarileştirilmesi için umut verici bir aday olduğu söylenebilir.

1. INTRODUCTION (GİRİŞ)

The rapid development of portable technology and the industrial revolution are rapidly increasing energy demands. The required energy is mainly obtained from fossil fuels, which have a much

higher consumption rate. However, fossil fuels consist of carbon that accumulates and causes environmental pollution as well as global warming. Also, other renewable energy sources such as solar, hydro and wind power are unstable and weather dependent. Therefore, dramatic climate

fluctuations, depletion of fossil fuels, environmental impacts and increasing energy demands force researchers to develop energy storage systems.

Electrochemical capacitor as an energy storage is gaining momentum with the growing demand for portable systems and hybrid electric vehicles that require instantaneous high-power density. Compared to secondary batteries, electrochemical capacitors, also known as supercapacitors (SCs), demonstrate higher power density, long life, wide thermal operating range and low maintenance cost [1]. SCs have two energy storage mechanisms: electrochemical double-layer capacitance (EDLCS) and pseudocapitance. Since electrochemical processes occur both at the surface and in bulk near the surface of the solid electrode, pseudocapacitors exhibit much greater capacitance and energy density than EDLCSs [2]. However, because of redox reactions occur at the electrode, electrodes that exhibit pseudocapacity are prone to swelling and shrinkage during the charge/discharge process, which can lead to poor mechanical stability and insufficient cycle stability. Therefore, the applicability of the pseudocapacity based supercapacitor is strongly dependent on the electrode material. An ideal electrode should have long cycle stability, large active surface area, a uniformly spaced morphology, high electrical conductivity, and rapid ion diffusion [3]. Generally, three types of electrode materials are studied in SCs: i) carbon-based materials, ii) metal oxides/sulphides and iii) conducting polymers [4]. Among these, conducting polymers have been attracted as electrode materials due to their electrochemical behaviours of fast reversible doping and de-doping ability, leading to storing the charges throughout the whole volume [5]. Mostly, because of high conductivity, simple processibility and high chemical stability, polypyrrole (PPy), polyaniline (PANI) and poly(3,4-ethylenedioxythiophene) (PEDOT) have been used for fabrication of electrodes employing in SCs. Especially, PPy is as an intrinsically conducting polymer has drawn more attention due to its great conductivity, high storage ability, high thermal and environmental durability, excellent redox ability [6]. However, as most conducting polymers, the PPy has a poorer long-term cycle stabilities than metal oxide, carbonaceous and metal sulphides since the redox spots in the polymer backbone are insufficiently stable and the backbone of polymer can be cracked after a few charge/discharge cycles.

Recently, to solve the cycling stability problem and improve capacitance of PPy based SCs, nanocomposite-based electrodes have been

designed by combining PPy with other materials such as metal oxides and metal sulphides [6–10]. Metal oxides are promising candidates for use as electrode materials in supercapacitors due to their high theoretical specific capacitance, low cost, and low toxicity. However, due to the low electrical conductivity of these materials (10^{-5} - 10^{-6} S/cm), the specific capacitance values are subject to a high deviation from their theoretical values [11]. Compared to these commonly used electrode materials, metal sulphides are abundant and inexpensive due to the presence of minerals in nature. More importantly, unlike metal oxides, metal sulphides generally exhibit higher electrical conductivity, flexibility, ionic diffusion, and anionic polarization due to the more covalent characteristics of the hard base O^{2-} ion being replaced by the soft base S^{2-}/S_2^{2-} ion [11–14]. In this regard, metal sulphides not only enhance the electronic properties but also improve the stability of PPy against to swelling and shrinking during the cyclic processes. For example, Peng et al., after synthesizing CuS (copper sulfide) by solvothermal method, obtained CuS/PPy composites at different ratios by in situ polymerization and used them as electrodes in supercapacitor [15]. In the study, the specific capacitance values at 1 A/g current density were recorded as 275, 212 and 427 F/g for pure PPy, CuS and CuS/PPy, respectively. After 1000 cycles, the initial capacity of PPy, CuS and CuS/PPy electrodes based SCs retained as 56%, 81% and 88%, respectively. In another study, Huo et al. synthesized the Co_3S_4 nanorod structure by hydrothermal method and obtained Co_3S_4 /PPy nanocomposite using in situ polymerization and applied it as an electrode in SC [16]. In the study, the R_{ct} values of Co_3S_4 and Co_3S_4 /PPy were determined as 0.78 and 0.48 Ω , respectively, indicating that Co_3S_4 increases ion diffusion and electrical conductivity of resulted composite. Also, because of the synergistic effect between Co_3S_4 and PPy, the specific capacitance of Co_3S_4 /PPy retained 98% of its initial capacitance value after 1000 cycles at current density of 8 A/g. In another study, Yan et al. prepared PPy/MoS₂/CC structured composite by synthesing MoS₂ nanosheets via hydrothermal method on carbon cloth (CC) then electrodeposition of PPy on MoS₂ nanosheets [17]. Electrochemical results reveal that the areal capacitance values of MoS₂/CC, PPy/CC and PPy/MoS₂/CC were 112.05, 648.49 and 1150.4 mF/cm², respectively. On the other hand, after 5000 times of charging/discharging cycles, the capacitance retention of MoS₂/CC, PPy/CC and PPy/MoS₂/CC electrodes were 71.5%, 58.3% and 87.2% respectively.

Herein, MnS rectangular prisms were synthesised via microwave-assisted method and coated on Ni foam (NF) by drop casting then MnS@PPy nanocomposite was prepared via electrodeposition of PPy on MnS rectangular prisms. Unlike to hydrothermal and solvothermal method, the MnS rectangular prisms have been synthesised in a very short time (2 h) via microwave-assisted method. Furthermore, electrodeposition of PPy directly on MnS@Ni foam remedied the need for any conductive additives (carbon allotropes etc.) and insulating binders, which reduces the internal resistance and provides faster charge transfer and high adhesion between the active material and the NF. In this research, to increase the electric conductivity, cycle life stability, electroactivity and capacitance of PPy, MnS for the first time have been incorporated into PPy matrix and resulting nanocomposite employed as cathode material for SCs. Electrochemical results reveal that MnS@PPy electrode exhibited a specific capacitance (C_s) of 1102 F/g which is approximately 5.6 times higher than that of the bare PPy (197 F/g). Furthermore, energy density (E_d) of the bare PPy was determined as 4.37 W/kg, by incorporation of MnS into PPy matrix the E_d value increased to 24.5 W/kg. On the other hand, after 1000 charge/discharge cycles, the cycle stability of the bare PPy remained at 72%, while MnS@PPy nanocomposite electrode is 95 %.

2. MATERIALS AND METHODS (MATERİYAL VE METOD)

2.1. Experimental Equipment (Deneysel Ekipman)

To synthesis MnS was used Milestone/FlexiWave Advanced Flexible Microwave Synthesis Platform. To define the phase type and crystalline structure, X-ray diffraction (XRD) patterns of MnS metal sulphide were investigating employing RIGAKU SmartLab. Surface morphology of the samples were investigated using TESCAN MAIA3 XMU scanning electron microscopy (SEM) instrument. Fourier transform infrared (FTIR) spectroscopy measurements of MnS, bare PPy and MnS@PPy were performed using the ATR method of Shimadzu spectrometer over a range from 400 to 4000 cm^{-1} . Thermal gravimetric analysis (TGA) was performed to examine the thermal properties of the samples. CV curves of samples were recorded using same set up for electrodeposition. Electrochemical impedance spectroscopy (EIS) and galvanic charge/discharge (GCD) cycles of bare PPy and MnS@PPy based SCs were recorded employing WonATech ZIVE SP1 potentiostat-galvanostat system with two electrodes.

2.2. Synthesis of MnS and MnS@PPy

Nanocomposite (MnS ve MnS@PPy Nanokompozitinin Sentezlenmesi)

12 mM of Manganese (II) acetate tetrahydrate was prepared in de-ionize (DI) water and stirred for 30 min. Next, 0.1 M polyvinylpyrrolidone (PVP, PVP10, MW ~ 10000) and 0.2 M Na_2S solution were prepared in DI water and subjected to magnetic stirrer for 45 min. Prepared two solutions were mixed and stirred for 2 min. Afterwards, the solution was subjected to 900-Watt microwave irradiation at 150 $^{\circ}\text{C}$ for 2 h and then cooled naturally to room temperature. The sample was then washed several times with DI water and ethanol, and the sample was finally dried at 60 $^{\circ}\text{C}$ overnight. Prior to deposition, to remove contamination from the surface of NF substrates (2x1 cm^2), they were cleaned using ultrasonic bath in 3 M HCl solution, acetone, and DI water respectively for 5 min. After that, the NF substrates were dried with N_2 gas flow and following at 60 $^{\circ}\text{C}$ for 2 h in an oven. To deposit MnS on NF substrate, 5 mg/mL of MnS was dispersed in a mixture of DI water and isopropoxide (3:1) via ultrasonication process (TEFIC TF-650 ultrasonication instrument). Afterwards, MnS solution was dropped on NF and following drying process on a heater at 60 $^{\circ}\text{C}$ for 10 min. This process was repeated 3 times and the obtained MnS/NF samples were finally dried at 60 $^{\circ}\text{C}$ overnight.

On the other hand, a potentiostat-galvanostat with standard three-electrode configuration was used for electrodeposition of PPy on surface of MnS@NF. The electrolyte solution for deposition of PPy was prepared by dissolving of 0.1 M pyrrole monomer and 0.1 M LiClO_4^- in DI water. Next, the PPy was directly electrodeposited via potentiostat-galvanostat system included Pt sheet, Ag/AgCl and MnS@NF as counter, reference and working electrodes, respectively on MnS@NF samples by cyclic voltammetry method in range of -0.2-1.1V. In addition, PPy was deposited on NF samples as control cathode with same potentiostat-galvanostat set up. Finally, the obtained samples were cleaned with DI water several times and dried at 60 $^{\circ}\text{C}$ overnight. To determine the amount of loaded cathode active materials, NF substrates were weighted via precision balance instrument before and after deposition of active materials. Finally, asymmetric SC (ASC) devices were manufactured in NF/MnS (or without)/PPy/Polypropylene separator/super carbon/NF structure, with 2 M KOH electrolyte (in DI water).

3. RESULTS (BULGULAR)

In Phase purity and crystallinity of MnS powder was analysed by X-ray diffraction (XRD). As seen in Figure. 1a, the diffraction patterns located at $2\theta = 29.7^{\circ}$, 34.4° , 49.4° , 58.7° ve 61.6° angles can be indexed to the (111), (200), (220), (311) and (222) orientations, respectively [18]. All the diffraction patterns agree well with the reported data of cubic phase of α -MnS crystals (JCPDS#88-2223) and no significant impurity peaks were observed [19]. Furthermore, one can see from the sharp and well-defined diffraction peaks, MnS metal sulphide which was synthesized using microwave assisted method presents a good crystallinity. The vibrational properties of MnS, PPy and MnS@PPy were investigated by FTIR spectra as shown in Figure 1b. The peak located at 1235 and 1008 cm^{-1} in the MnS spectrum can be assigned to the formation of complex sulphur with the active sites in MnS. The peak at 610 cm^{-1} is ascribed to the Mn-S stretching vibration, indicating that MnS is successfully synthesised with microwave assisted method [9,20]. Moreover, in the spectrum of PPy, the peaks appeared at 1540 and 1453 cm^{-1} stem from the C-C and C-N stretching vibration of the pyrrole ring. The bands located at 1285 , 1170 and 1030 cm^{-1} are assigned to the C=N bending, C-N stretching and =C-H in-plane vibrations of PPy rings, respectively [21]. The peak at 678 cm^{-1} is related with C-H deformational vibration-mode of the PPy. In case of MnS@PPy nanocomposite, all the characteristic peaks of PPy can be seen in the spectrum. In addition, a new peak appeared approximately at 600 cm^{-1} , exhibiting that MnS is incorporated into PPy matrix. Furthermore, the bands seen at 1540 , 1453 , 1285 , 1030 and 678 cm^{-1}

in the spectrum of bare PPy are observed at slightly lower wavenumbers in the spectrum of MnS@PPy nanocomposite at 1521 , 1436 , 1280 , 1022 and 673 cm^{-1} , respectively. The observed shifting in characteristic bands of PPy with incorporation of MnS exhibits the electronic/synergistic interaction working at molecular degrees [21–23]. So, it can be said that MnS@PPy nanocomposite is successfully prepared by electro-polymerization of pyrrole on MnS/NF.

To assess the effects of MnS on thermal properties of PPy, TGA measurements were conducted and the obtained TGA curves are exhibited in Figure 1c. The standard thermograms for bare PPy, MnS and MnS@PPy nanocomposite show a three-step weight loss process as depicted in Figure 1c. The first step weight loss occurred between 28 - $180\text{ }^{\circ}\text{C}$ stem from the evaporative loss of water and other volatile impurities [24]. The second step weight loss aroused between 180 - $385\text{ }^{\circ}\text{C}$ in bare PPy and MnS@PPy due to gradual thermal decomposition of the polymer chains [25]. The second step weight loss occurred for MnS between 180 - $550\text{ }^{\circ}\text{C}$ due to the decomposition of sulphur in MnS structure. The third weight loss taken place between 385 - $1000\text{ }^{\circ}\text{C}$ can be attributed to pyrolysis of the materials. As deduced from TGA plots, bare PPy exhibited around 30.8% weight loss at $385\text{ }^{\circ}\text{C}$ which reduced to 24.5% for MnS@PPy. The reducing in weight loss of nanocomposite indicated that the thermal stability of PPy was significantly improved due to the intervening MnS in the polymer chains [26]. This caused in prolonged degradation of PPy chains, resulting in the increased thermal stability of the nanocomposite.

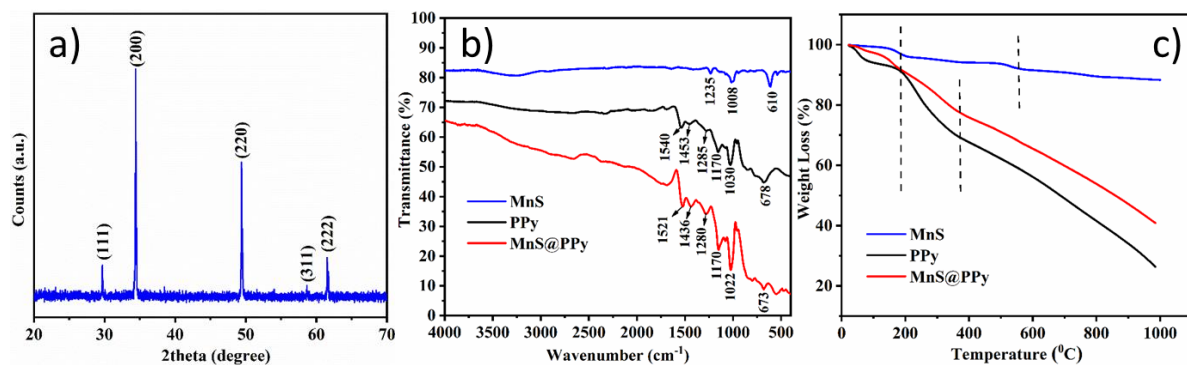


Figure 1. (a) XRD pattern of MnS, (b) FTIR spectra and (c) TGA curves of MnS, PPy and MnS@PPy nanocomposite ((a) *MnS'nin XRD kırınımları*, *MnS*, *PPy* ve *MnS@PPy* nanokompozitinin (b) *FTIR spektrumları* ve (c) *TGA eğrileri*)

Figure 2 exhibits the EDS and EDS mapping of MnS metal sulphide, top view SEM micrographs of MnS, bare PPy and MnS@PPy nanocomposite. As shown in Figure 2a, atomic percentage of

manganese and sulphur elements is 49.2 and 50.8% , respectively. In ideal case, the atomic percentage of Mn and S could be equal, the ratio of Mn/S is 0.97 which is very close to ideal number. Furthermore,

EDS mapping reveal that Mn and S elements homogenously distributed in MnS. EDS results are in good agreement with XRD patterns which are confirming that MnS successfully are synthesised using microwave assisted method in 2 h. As seen in Fig. 2c, the morphology of MnS metal sulphide consists of 500 nm wide cubes and 200 μm long rectangle prisms. In addition, it is seen that there is no formation other than cubic and prismatic structures. As shown in Figure 2d, the morphology of the PPy polymer consists of spherical grains with dimensions of about 400 nm. Moreover, it is observed that the spherical structures are interconnected and densely packed. Figure 2e dedicates that MnS@PPy nanocomposite firmly adhered to NF substrate without insulating adhesive. When Figure 2f is examined, the morphology of the nanocomposite structure consists of both cubic and prismatic MnS structures and spherical grains of PPy polymer. Therefore, it can

be said that the MnS@PPy nanocomposite was successfully synthesized using electrochemical polymerization method. Furthermore, incorporation of MnS changed the growth dynamics of PPy, leading that formation of PPy as nano sheets on MnS structures. This indicates that the active surface area of the resulted nanocomposite structure has increased significantly and PPy bounded with MnS rectangular prisms strongly. The enlargement of the surface area provides many advantages for the SC. First, it provides adequate surface contact between the electrode and electrolytes and accelerates the Faraday reactions as well as increases the reaction rate [27]. Second, it makes a large amount of electrolyte accessible for faster mass transfer [28]. Third, increasing the specific surface area promotes high mechanical flexibility, thereby reducing pulverization of electroactive materials during difficult cycle performance [29].

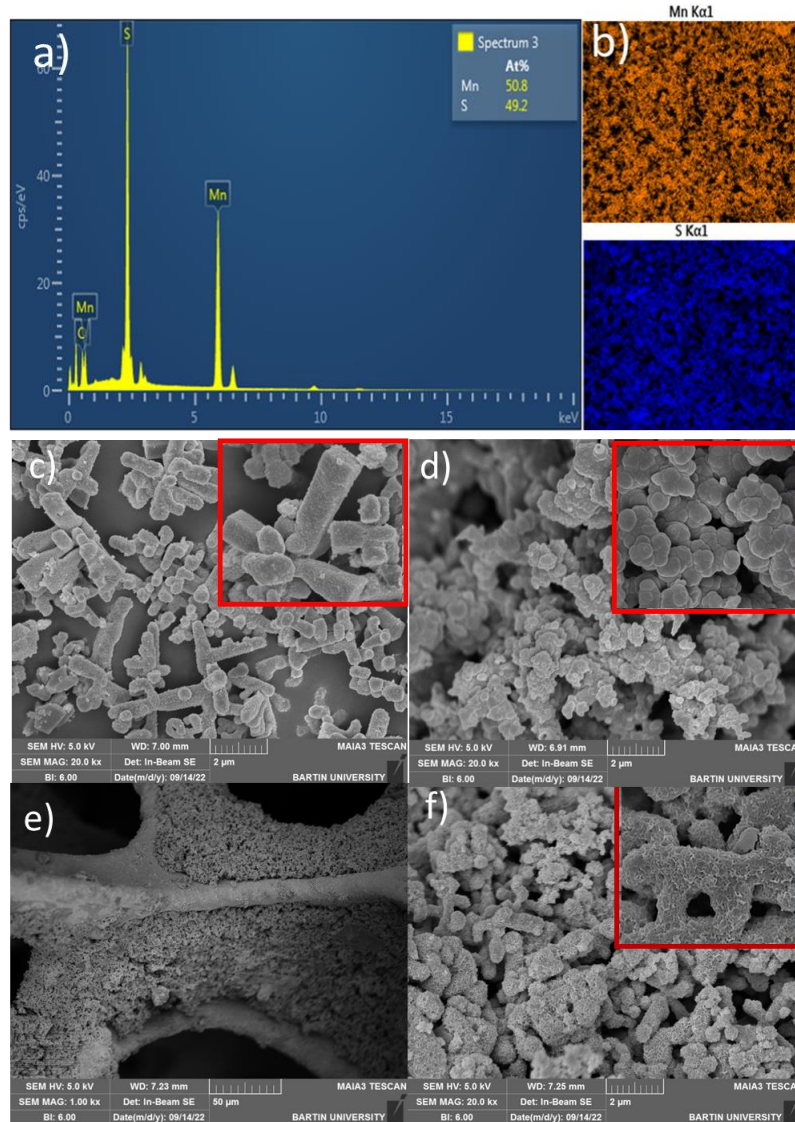


Figure 2. (a) EDS and (b) EDS mapping of MnS, SEM micrographs of (c) MnS, (d) bare PPy, (e) and (f) MnS@PPy nanocomposite with low and high magnifications, respectively (*MnS'nin (a) EDS ve (b) EDS haritalaması, (c) MnS, (d) saf PPy ve (f) MnS@PPy nanokompozitinin sırasıyla düşük ve yüksek çözünürlüklü SEM görüntüleri*)

The electrochemical behaviour of PPy and MnS@PPy nanocomposite was investigated in a 2M KOH aqueous electrolyte with a two-electrode potentiostat-galvanostat system. Cyclic voltammetry (CV), galvanic charge/discharge cycles (GCD), electrochemical impedance spectroscopy (EIS) and cycle stability measurements were performed for each electrode. CV measurements were carried out between 0 and 0.5 V at a scanning rate of 20 mV/s, GCD curves were recorded at different current densities (1A/g, 2A/g, 3A/g, 4A/g and 5 A/g) between 0 and 0.4 V, EIS curves were performed between 100 kHz-0.01 Hz and cycle stabilities of bare PPy and MnS@PPy electrode based SCs were taken as 1000 cycles at a current density of 2A/g. Figure 3 shows the electrochemical performances of SCs fabricated with bare PPy and MnS@PPy nanocomposite. Clearly, a double redox peak is observed in all CV curves over the 0-0.4 V voltage window, indicating pseudocapacitive properties [30]. When Figure 3a is examined, the oxidation and reduction peak current densities of the PPy were 25 and 17 mA/cm², while by introduction of MnS into the PPy polymer matrix, the peak current densities reached to 121 and 107 mA/cm², respectively. Moreover, the redox peak positions changed, and the peak-to-peak distance increased significantly compared to PPy. This indicates that MnS dramatically increases the electron transfer rate and speed [31]. Moreover, it indicates that the nanocomposite electrode will show a larger capacitance and lower internal resistance than the bare polymer [32]. Also, compared to PPy, MnS@PPy shows larger CV integrated areas, indicating higher electrochemical capacitance. The remarkable increase in the electrochemical properties of the MnS@PPy nanocomposite compared to the bare PPy is due to the increase in the electrical conductivity of the resulted nanocomposite by acting as a bridge between the PPy chains of the MnS rectangular prisms and the enlargement of the specific surface area by differentiating the surface morphology [33]. Figure 3b-c show the GCD curves of the PPy and MnS@PPy electrodes at different current densities, respectively. During fast charging and discharging, the internal resistance in the discharge curves shows a negligible internal resistance due to diffusion of electrolyte ions. When the current densities are increased, the shape and size of the charge-discharge curve remain the same, indicating stable behaviour of the electrode. The specific capacitance (C_{sp}) of the electrode from the charge-discharge curves was calculated with the following equation.

$$C_{sp} = (I \Delta t) / (m \Delta V)$$

Here, “I, Δt , m and ΔV represents the discharge current, the discharge time, the weight of the material coated on the NF substrates and potential window, respectively. Furthermore, energy density (E_d) and power density (P_d) of the electrodes were determined according to the following equations.

$$E_d = \frac{1}{2} C_{sp} V^2 \quad \text{and} \quad P_d = \frac{1}{2} C_{sp} V \cdot s$$

The determined C_{sp} values decrease with increasing scanning rate. This is because charge and discharge processes occur very quickly at higher scanning rates. Therefore, ions cannot penetrate deep into the electrode, resulting in low specific capacitance. From the GCD curves, the C_{sp} values of the PPy and MnS@PPy electrodes at 1 A/g current density were obtained as 197 and 1102 F/g, respectively. The C_{sp} value was increased approximately 5.6 times with incorporation of MnS into PPy. In addition, the energy (E_d) and power densities (P_d) of PPy and MnS@PPy were determined as 4.37 and 24.5 W/kg and 199.5 and 200 Wh/kg, respectively. These enhancements can be attributed to the increase of the electron transfer rate and speed, as well as the expansion of the surface area. Moreover, it is clear from these results that the specific capacitance of MnS@PPy nanocomposite compared to PPy shows excellent storage capacity even at higher current densities.

As shown in Figure 3d, EIS analyses were performed to further investigate the electrochemical performance of the electrodes. Nyquist plots of all electrodes show a single semicircle in the high frequency domain and a curved line in the low frequency domain. The diameter of the semicircle represents the charge transfer resistance (R_{ct}), which can reflect the permeability of the electrolyte. The linear parts correspond to the Warburg impedance (W), which can represent the ion diffusion resistance. Also, the value at which the curve crosses the x-axis represents the equivalent series resistance (R_s), which includes the internal resistance, the contact resistance of the interface (electrolyte/electrode), and the ionic resistance of the electrolyte [34]. When Figure 3d is examined, it is observed that PPy has higher R_{ct} , R_s and W values compared to MnS@PPy nanocomposite. This shows that the MnS@PPy nanocomposite has excellent electron transfer kinetics, low energy loss, and higher diffusion of the electrolyte on the electrode surface compared to the pure polymer. EIS analysis results support each other with CV and GCD measurements.

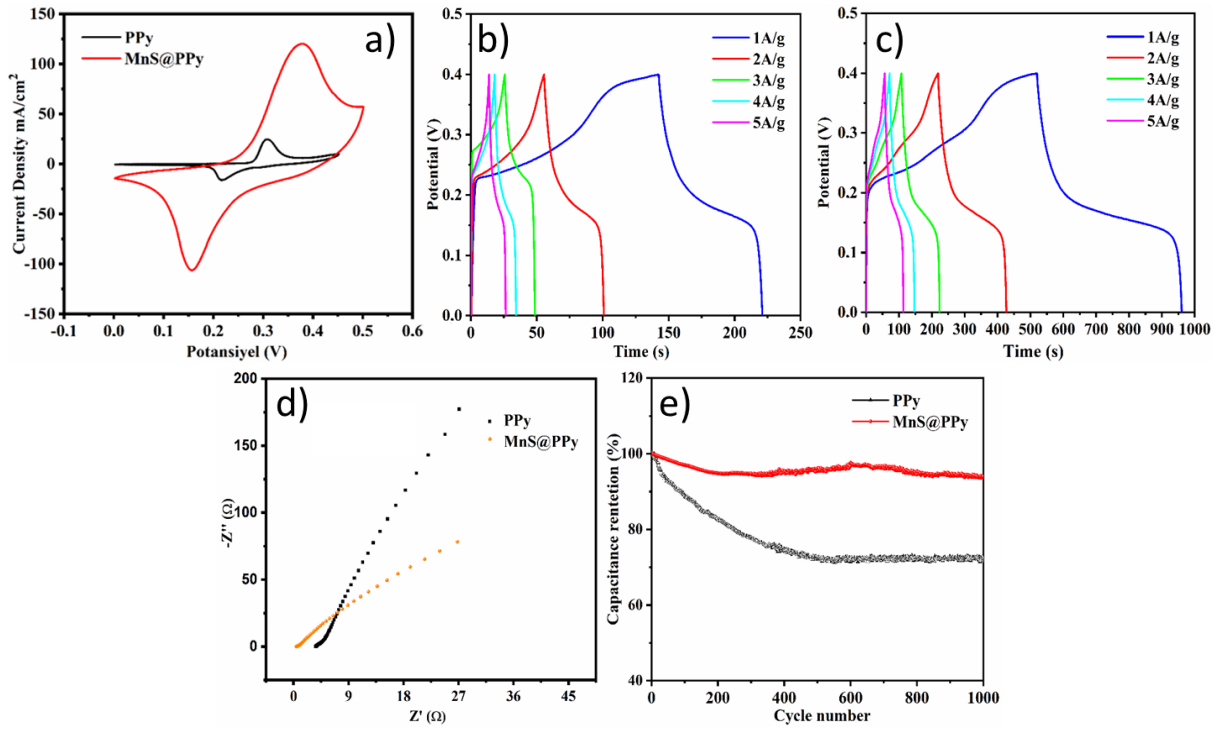


Figure 3. (a) CV curves of electrodes (b) and (c) GCD plots of bare PPy and MnS@PPy at different current densities, respectively (d) EIS and (e) cycle stabilities of bare PPy and MnS@PPy nanocomposite ((a) elektrotların CV eğrileri, (b) ve (c) sırasıyla, saf PPy and MnS@PPy'nin farklı akım yoğunluklarında ölçülen GCD eğrileri, saf PPy and MnS@PPy nanokompozitin (d) EIS ve (e) döngü kararlılıkları)

For practical applications of SCs, capacity retention against number of cycles is an important parameter to consider. As seen in Figure 3e, the specific capacitance of PPy decreased to 72% from its initial value after 1000 cycles, while that of MnS@PPy nanocomposite remain as 95%. The introduction of MnS into the PPy matrix not only increased the electrochemical activity but also significantly increased the cycling stability due to the improvement of stability against to shrinking or swelling.

4. CONCLUSIONS (SONUÇLAR)

In briefly, rectangular prism shaped MnS metal sulphide was successfully synthesized by microwave assisted method and MnS@PPy nanocomposite was fabricated directly on NF substrate by electropolymerization method. In this way remedied the need for any conductive additives and insulating binders, which reduces the internal resistance and provides faster charge transfer and high adhesion between the active material and the NF. Moreover, because of the introduction of MnS rectangular prisms into the nanocomposite system, the nucleation and growth kinetics of the PPy polymer differed and the specific surface area expanded as well as the charge transfer kinetics and conductivity improved. Electrochemical results show that MnS@PPy electrode exhibited a specific

capacitance (C_s) of 1102 F/g which is approximately 5.6 times higher than that of the bare PPy (197 F/g). Furthermore, energy density (E_d) of the bare PPy was determined as 4.37 W/kg, by incorporation of MnS into PPy matrix the E_d value increased to 24.5 W/kg. More importantly, after 1000 charge/discharge cycles, the cycle stability of the bare PPy remained at 72%, while that of MnS@PPy nanocomposite electrode recorded as 95 % due to the improvement of PPy stability against to swelling and shrinking during the charge-discharge process. In the light of the results obtained from current study, it is clearly seen that MnS@PPy structured nanocomposite is a promising candidate for SC applications.

ACKNOWLEDGMENTS (TEŞEKKÜR)

This work was supported by Scientific Research Foundation of Bartın University under project No. 2020-FEN-A-020. / Bu çalışma Bartın Üniversitesi Bilimsel Araştırma Projeleri Birimi tarafından 2020-FEN-A-020 numaralı proje kapsamında desteklenmiştir.

DECLARATION OF ETHICAL STANDARDS (ETİK STANDARTLARIN BEYANI)

The author of this article declares that the materials and methods they use in their work do not require

ethical committee approval and/or legal-specific permission.

Bu makalenin yazarı çalışmalarında kullandıkları materyal ve yöntemlerin etik kurul izni ve/veya yasal-özel bir izin gerektirmediğini beyan ederler.

AUTHORS' CONTRIBUTIONS (YAZARLARIN KATKILARI)

Mahir GÜLEN: He conducted the experiments, analyzed the results and performed the writing process.

Deneyleri yapmış, sonuçlarını analiz etmiş ve maklenin yazım işlemini gerçekleştirmiştir.

CONFLICT OF INTEREST (ÇIKAR ÇATIŞMASI)

There is no conflict of interest in this study.

Bu çalışmada herhangi bir çıkar çatışması yoktur.

REFERENCES (KAYNAKLAR)

- [1] S. Unknown, P. Chand, A. Joshi, Biomass derived carbon for supercapacitor applications: Review, *J Energy Storage*. 39 (2021) 102646. <https://doi.org/10.1016/j.est.2021.102646>.
- [2] A. Karimi, I. Kazeminezhad, L. Naderi, S. Shahrokhian, Construction of a Ternary Nanocomposite, Polypyrrole/Fe-Co Sulfide-Reduced Graphene Oxide/Nickel Foam, as a Novel Binder-Free Electrode for High-Performance Asymmetric Supercapacitors, *The Journal of Physical Chemistry C*. 124 (2020) 4393–4407. <https://doi.org/10.1021/acs.jpcc.9b11010>.
- [3] Y.F. Fan, Z.L. Yi, G. Song, Z.F. Wang, C.J. Chen, L.J. Xie, G.H. Sun, F.Y. Su, C.M. Chen, Self-standing graphitized hybrid Nanocarbon electrodes towards high-frequency supercapacitors, *Carbon N Y*. 185 (2021) 630–640. <https://doi.org/10.1016/J.CARBON.2021.09.059>.
- [4] Z. Yu, L. Tetard, L. Zhai, J. Thomas, Supercapacitor electrode materials: nanostructures from 0 to 3 dimensions, *Energy Environ Sci*. 8 (2015) 702–730. <https://doi.org/10.1039/C4EE03229B>.
- [5] Q. Meng, K. Cai, Y. Chen, L. Chen, Research progress on conducting polymer based supercapacitor electrode materials, *Nano Energy*. 36 (2017) 268–285. <https://doi.org/10.1016/J.NANOEN.2017.04.040>.
- [6] H. Ji, C. Zhang, W. Rao, B. Guo, L. Fan, Z. Bai, H. Bao, J. Xu, Eco-friendly Polypyrrole-coated Cocozelle Composites for Supercapacitor Application, *Fibers and Polymers*. 21 (2020) 1300–1307. <https://doi.org/10.1007/s12221-020-9375-0>.
- [7] I.K. Durga, S.S. Rao, R.M.N. Kalla, J.W. Ahn, H.J. Kim, Facile synthesis of FeS₂/PVP composite as high-performance electrodes for supercapacitors, *J Energy Storage*. 28 (2020). <https://doi.org/10.1016/J.EST.2020.101216>.
- [8] F. Hamidouche, M.M.S. Sanad, Z. Ghebache, N. Boudieb, Effect of polymerization conditions on the physicochemical and electrochemical properties of SnO₂/polypyrrole composites for supercapacitor applications, *J Mol Struct*. 1251 (2022). <https://doi.org/10.1016/J.MOLSTRUC.2021.131964>.
- [9] R. BoopathiRaja, M. Parthibavarman, Desert rose like heterostructure of NiCo₂O₄/NF@PPy composite has high stability and excellent electrochemical performance for asymmetric super capacitor application, *Electrochim Acta*. 346 (2020). <https://doi.org/10.1016/J.ELECTACTA.2020.136270>.
- [10] J. Hao, H. Liu, S. Han, J. Lian, MoS₂ Nanosheet-Polypyrrole Composites Deposited on Reduced Graphene Oxide for Supercapacitor Applications, *ACS Appl Nano Mater*. 4 (2021) 1330–1339. <https://doi.org/10.1021/acsanm.0c02899>.
- [11] X. Lu, T. Zhai, X. Zhang, Y. Shen, L. Yuan, B. Hu, L. Gong, J. Chen, Y. Gao, J. Zhou, Y. Tong, Z.L. Wang, WO_{3-x}@Au/MnO₂ core-shell nanowires on carbon fabric for high-performance flexible supercapacitors, *Advanced Materials*. 24 (2012) 938–944. <https://doi.org/10.1002/adma.201104113>.

- [12] T. Yi, S. Qi, Y. Li, L. Qiu, Y. Liu, Y. Zhu, J. Zhang, Y. Li, Facile Synthesis of Sheet Stacking Structure NiCo₂S₄@PPy with Enhanced Rate Capability and Cycling Performance for Aqueous Supercapacitors, *Energy Technology*. 8 (2020) 1–13. <https://doi.org/10.1002/ente.202000096>.
- [13] S. Cheng, T. Shi, C. Chen, Y. Zhong, Y. Huang, X. Tao, J. Li, G. Liao, Z. Tang, Construction of porous CuCo₂S₄ nanorod arrays via anion exchange for high-performance asymmetric supercapacitor OPEN, (2017). <https://doi.org/10.1038/s41598-017-07102-1>.
- [14] C.H. Lai, M.Y. Lu, L.J. Chen, Metal sulfide nanostructures: synthesis, properties and applications in energy conversion and storage, *J Mater Chem*. 22 (2011) 19–30. <https://doi.org/10.1039/C1JM13879K>.
- [15] H. Peng, G. Ma, K. Sun, J. Mu, H. Wang, Z. Lei, High-performance supercapacitor based on multi-structural CuS@polypyrrole composites prepared by in situ oxidative polymerization, *J Mater Chem A Mater*. 2 (2014) 3303–3307. <https://doi.org/10.1039/c3ta13859c>.
- [16] W. Huo, X. Zhang, X. Liu, H. Liu, Y. Zhu, Y. Zhang, J. Ji, F. Dong, Y. Zhang, Construction of advanced 3D Co₃S₄@PPy nanowire anchored on nickel foam for high-performance electrochemical energy storage, *Electrochim Acta*. 334 (2020). <https://doi.org/10.1016/J.ELECTACTA.2020.135635>.
- [17] X. Yan, J. Miao, J. Wang, H. Jiang, M. You, Y. Zhu, J. Pan, High-performance polypyrrole coated MoS₂ nanosheets grown on carbon cloth as electrodes for flexible all-solid-state symmetric supercapacitor, *Mater Sci Eng B Solid State Mater Adv Technol*. 269 (2021). <https://doi.org/10.1016/J.MSEB.2021.115166>.
- [18] R. Wei, Y. Dong, Y. Zhang, X. Kang, X. Sheng, J. Zhang, Hollow cubic MnS-CoS₂-NC@NC designed by two kinds of nitrogen-doped carbon strategy for sodium ion batteries with extraordinary rate and cycling performance, *Nano Res*. 15 (2022) 3273–3282. <https://doi.org/10.1007/s12274-021-3973-z>.
- [19] Q. Liu, S.J. Zhang, C.C. Xiang, C.X. Luo, P.F. Zhang, C.G. Shi, Y. Zhou, J.T. Li, L. Huang, S.G. Sun, Cubic MnS-FeS₂ Composites Derived from a Prussian Blue Analogue as Anode Materials for Sodium-Ion Batteries with Long-Term Cycle Stability, *ACS Appl Mater Interfaces*. 12 (2020) 43624–43633. <https://doi.org/10.1021/acscami.0c10874>.
- [20] Z.K. Heiba, M.B. Mohamed, S.I. Ahmed, A.M. El-naggar, A. Albassam, Effect of composition ratio on the structural and optical properties of MnS@ZnS nanocomposites, *Journal of Materials Science: Materials in Electronics*. 31 (2020) 14746–14755. <https://doi.org/10.1007/s10854-020-04038-7>.
- [21] Y. Chen, W. Ma, K. Cai, X. Yang, C. Huang, In Situ Growth of Polypyrrole onto Three-Dimensional Tubular MoS₂ as an Advanced Negative Electrode Material for Supercapacitor, *Electrochim Acta*. 246 (2017) 615–624. <https://doi.org/10.1016/J.ELECTACTA.2017.06.102>.
- [22] N.A. Niaz, A. Shakoor, M. Imran, N.R. Khalid, F. Hussain, H. Kanwal, M. Maqsood, S. Afzal, Enhanced electrochemical performance of MoS₂/PPy nanocomposite as electrodes material for supercapacitor applications, *Journal of Materials Science: Materials in Electronics*. 31 (2020) 11336–11344. <https://doi.org/10.1007/s10854-020-03682-3>.
- [23] S. Ahmad, I. Khan, A. Husain, A. Khan, A.M. Asiri, Properties of Polypyrrole / MoS₂ Nanocomposite, (2020) 1–13.
- [24] A. Husain, S.A. Al-Zahrani, A. Al Otaibi, I. Khan, M.M.A. Khan, A.M. Alosaimi, A. Khan, M.A. Hussein, A.M. Asiri, M. Jawaid, Fabrication of reproducible and selective ammonia vapor sensor-pellet of

- polypyrrole/cerium oxide nanocomposite for prompt detection at room temperature, *Polymers* (Basel). 13 (2021). <https://doi.org/10.3390/polym13111829>.
- [25] S. Abdi, M. Nasiri, A. Mesbahi, M.H. Khani, Investigation of uranium (VI) adsorption by polypyrrole, *J Hazard Mater.* 332 (2017) 132–139. <https://doi.org/10.1016/J.JHAZMAT.2017.01.013>.
- [26] L. Seid, D. Lakhdari, M. Berkani, O. Belgherbi, D. Chouder, Y. Vasseghian, N. Lakhdari, High-efficiency electrochemical degradation of phenol in aqueous solutions using Ni-PPy and Cu-PPy composite materials, *J Hazard Mater.* 423 (2022). <https://doi.org/10.1016/J.JHAZMAT.2021.126986>.
- [27] X. Xiong, J. Chen, D. Zhang, A. Li, J. Zhang, X. Zeng, Hetero-structured nanocomposites of Ni/co/O/S for high-performance pseudo-supercapacitors, *Electrochim Acta.* 299 (2019) 298–311. <https://doi.org/10.1016/J.ELECTACTA.2018.12.178>.
- [28] S. Kumar, S. Riyajuddin, M. Afshan, S.T. Aziz, T. Maruyama, K. Ghosh, In-Situ Growth of Urchin Manganese Sulfide Anchored Three-Dimensional Graphene (γ -MnS@3DG) on Carbon Cloth as a Flexible Asymmetric Supercapacitor, *Journal of Physical Chemistry Letters.* 12 (2021) 6574–6581. <https://doi.org/10.1021/acs.jpcllett.1c01553>.
- [29] S.C. Song, D.C. Zuo, C.S. An, X.H. Zhang, J.H. Li, Z.J. He, Y.J. Li, J.C. Zheng, Self-assembled GeOX/Ti₃C₂TX Composites as Promising Anode Materials for Lithium Ion Batteries, *Inorg Chem.* 59 (2020) 4711–4719. <https://doi.org/10.1021/acs.inorgchem.9b03784>.
- [30] T. Xu, G. Li, X. Yang, Z. Guo, L. Zhao, Design of the seamless integrated C@NiMn-OH-Ni₃S₂/Ni foam advanced electrode for supercapacitors, *Chemical Engineering Journal.* 362 (2019) 783–793. <https://doi.org/10.1016/J.CEJ.2019.01.083>.
- [31] Y. Wang, J. Huang, Y. Xiao, Z. Peng, K. Yuan, L. Tan, Y. Chen, Hierarchical nickel cobalt sulfide nanosheet on MOF-derived carbon nanowall arrays with remarkable supercapacitive performance, *Carbon N Y.* 147 (2019) 146–153. <https://doi.org/10.1016/J.CARBON.2019.02.082>.
- [32] S. Liu, K.S. Hui, K.N. Hui, 1 D Hierarchical MnCo₂O₄ Nanowire@MnO₂ Sheet Core–Shell Arrays on Graphite Paper as Superior Electrodes for Asymmetric Supercapacitors, *ChemNanoMat.* 1 (2015) 593–602. <https://doi.org/10.1002/cnma.201500105>.
- [33] K.Y. Yasoda, S. Kumar, M.S. Kumar, K. Ghosh, S.K. Batabyal, Fabrication of MnS/GO/PANI nanocomposites on a highly conducting graphite electrode for supercapacitor application, *Mater Today Chem.* 19 (2021). <https://doi.org/10.1016/J.MTCHEM.2020.100394>.
- [34] X. Li, M. Zhang, L. Wu, Q. Fu, H. Gao, Annealing temperature dependent ZnCo₂O₄ nanosheet arrays supported on Ni foam for high-performance asymmetric supercapacitor, *J Alloys Compd.* 773 (2019) 367–375. <https://doi.org/10.1016/J.JALLCOM.2018.09.197>.